USAGE OF AN AUTOMATED THREE-STUB WATER-LOADED IMPEDANCE GENERATOR FOR RBF CALIBRATION OF A WAVEGUIDE TEN-PORT REFLECTOMETER

USAGE OF AN AUTOMATED THREE-STUB WATER-LOADED IMPEDANCE GENERATOR FOR RBF CALIBRATION OF A WAVEGUIDE TEN-PORT REFLECTOMETER

Juan Monzó-Cabrera, Juan Luis Pedreño-Molina, Antonio José Lozano-Guerrero, Francisco Javier Clemente-Fernández, and Alejandro Díaz-Morcillo

Departamento de Tecnologías de la Información y las Comunicaciones
Universidad Politécnica de Cartagena
Cartagena, Spain

email: juan.monzo@upct.es

Fax: +34 968 32 5973

ABSTRACT: *In this work, a waveguide impedance generator based on the use of three motor-controlled metallic stubs, a monomode cavity loaded with water and PTFE cylinders is used in order to calibrate a waveguide ten-port reflectometer. RBF neural networks are used in order to learn the relationship between the actual reflection coefficient and the power detectors' output. Results indicate that this impedance generator can be successfully used in order to calibrate the ten-port reflectometer.*

Key words: *reflectometer; impedance generator; calibration; waveguide; RBF neural network*

1. INTRODUCTION

Traditional methods for the estimation of the reflection coefficient in waveguides are based, for example, in slotted lines or impedance bridges [1] or circuit designs based on directional couplers [2]. Another possibility is the so-called six-port reflectometer [3-4] or the employment of conventional network analyzers. The six-port, designed by Hoer in 1972, is an inexpensive device that avoids the use of network analyzers since it is based on the employment of simple power detectors (like diodes or thermistors) [5-6]. Due to several effects, such as noise and the non-linearity characteristics of the power detectors, a calibration procedure has to be carried out for the six-port working frequencies to ensure the accuracy of the measurements.

Recently, a waveguide ten-port reflectometer has been presented [7-8] as an alternative to six-port configuration. This new design and the incorporated neural network calibration allow to avoid problems caused by the non-linearity of the detectors, and to get robustness, flexibility and adaptability characteristics for this device. For instance, the ten-port configuration is able to keep on measuring even when some of the detectors are broken. Additionally, it offers phase measurements without needing phase detection [7-8]. However, the main drawback of the calibration process based in neural networks is that many calibration data must be produced in order to achieve good calibration levels. Therefore, it is necessary to implement a device capable of providing different reflection coefficients from adapted values to highly reflective ones.

In this work we present a new waveguide automated impedance generator based on the use of three cylindrical metallic stubs and a water load surrounded by a cylindrical PTFE cast. This device allows a proper sweep of the entire Smith Chart by means of mobile metallic stubs driven by step motors. The combination of this automated impedance generator and the RBF neural network calibration leads to very accurate results for the ten-port reflectometer performance both in magnitude and phase.

2. THEORY FOR TEN-PORT AND IMPEDANCE GENERATION

2.1 Ten-Port Description

The ten-port reflectometer has been studied in detail in previous works [7-8]. As in previous cases, it consists of a standard WR-340 waveguide section (4.34 cm x 8.68 cm) that contains eight equally spaced coaxial probes inserted at the center of the wide wall of the waveguide. These coaxial probes sample the standing wave within the waveguide and therefore provide an estimation of the complex reflection coefficient both in magnitude and phase. Each output of these coaxial probes is connected to a non-linear low-cost Linear Technology LTC5530 power meter.

Figure 1 shows the scheme of the proposed configuration where Ports 1 and 2 are respectively connected to the vector network analyzer and impedance generator. Ports ranging from 3 to 10 correspond to the ports of coaxial probes. The central conductor of the SMA coaxial connectors penetrates inside the rectangular cross section with a length of 16 mm, which provides a power coupling of -23dB. This value has been chosen in order to ensure that the power detectors are never saturated since the output power of the network analyzer, which was used in this work as the microwave source and

reference instrument, was set to 27 dBm and the saturation power level of the power detectors is 10 dBm. The distance between each coaxial port is selected as function of the TE_{10} wavelength, resulting in 22 mm, with separations of 35 mm from both ends. The final length of the ten-port is 222 mm [7-8].

2.2 Automated Impedance Generator

Figure 2 shows a scheme with the dimensions of the proposed impedance generator. The inner dimensions of the metallic casing correspond to a WR-340 waveguide. Three metallic screws with 2 cm diameter are mounted at the upper wall of the waveguide. These screws act as reactive stubs whose impedances depend on the inserted length within the waveguide. A cavity was implemented by using a vertical 2 mm thick metallic iris, an inner 2 cm diameter water cylinder and a PTFE cylinder with inner radius of 2 cm and outer radius of 3.85 cm.

Three USB-controlled RS 440-420 step motors were used in order to insert the screws within the waveguide up to a defined length. Both the complex reflection coefficient measured by the network analyzer and the eight scalar power detector outputs were collected for each position of the three metallic screws. These data were used in order to train and test the neural networks used during the calibration procedure.

2.3 Neural Network Calibration Procedure

A conventional Radial Basis Function (RBF) neural network has been used in order to calibrate the ten-port reflectometer due to its simplicity [7]. In this case, the input vector is formed by the eight voltage values provided by the power detectors whereas the output of the network estimates $|S_{11}|$. A similar RBF configuration is used in order to estimate S_{11} phase [7-8].

The procedure shown in [7] has been applied here in order to train the RBF neural networks for both S_{11} phase and magnitude. However, as a difference with [7-8] in this work the generation of different S_{11} complex values has been accomplished by means of the three stub impedance generator. The movement of the three metallic screws provided changes in the reflection coefficient allowing controlled and repetitive values all around the Smith Chart.

Microwave power was supplied by a ZVRE Rohde & Schwarz vector network analyzer (VNA) that acted as the microwave source and provided the S_{11} reference values for RBF network training. Thus, these reference values were used as the desired output values of the RBF neural network during the training stage. Some of these measured reflection coefficients, which were not used during the training stage, were employed for validation purposes [7-8].

3. EXPERIMENTAL SET UP

Figure 3 shows the experimental set up implemented for the ten-port calibration and validation. The three stub impedance generator has been employed for testing the sensor under low power conditions, and to provide different S_{11} values for calibration and validation purposes.

Two DC supply sources were employed for biasing the eight LTC5530 power sensors. A DT9800-EC data acquisition board was used in order to obtain the output voltage values of the power sensors for each position of the tuning screws.

The ZVRE VNA provided a 2.45 GHz signal with a power level of 27 dBm. This instrument was also used for collecting the actual values of the reflection coefficient. Therefore the ten-port reflectometer was trained at this frequency value. Once the ten-port was calibrated, the VNA was no longer necessary and the ten-port could operate autonomously.

The personal computer was connected to the VNA by a USB-GPIB communication board, and to the data acquisition board through conventional USB connectors. The error for RBF training was obtained by comparing the reference S_{11} value provided by the VNA and the value computed by the neural network when using the eight power sensor outputs as input values [7].

4. RESULTS

Figure 4 shows the reflection coefficient data obtained by the VNA for different positions of the impedance generator's metallic stubs. As it can be observed from these data, the impedance generator was able to provide results all around the Smith Chart and, thus, allowed a proper RBF neural network training.

Figure 5 shows the data employed for training and validating the RBF neural network. As it can be observed, different data groups were employed for calibration and validation. In this case 200 complex reflection coefficient values were used for training purposes whereas 200 complex values, different from training ones, were used for validating the proposed calibration procedure.

The comparison between the reference value for the reflection coefficient magnitude provided by the VNA and the value obtained by the ten-port reflectometer is depicted in Figure 6. This representation follows a straight line with slope 1 in a very closely way. A neural network with 200 neurons and 200 training values was used. The usage of less neurons or training points made the ten-port performance worse.

Figure 7 shows the response of the phase estimation for the reflection coefficient versus the reference value when using 200 neurons and 200 training phase values. As in the previous case, a good correlation was obtained between VNA measurements and ten-port estimations. In both Figures 6 and 7, the data used for validation purposes were different from that used during RBF training.

5. CONCLUSIONS

A new RBF calibration procedure for the ten-port waveguide reflectometer based in the usage of an automated three-stub water-loaded impedance generator has been described. The impedance generator was able to produce repetitive values all around the Smith Chart, which allowed proper training values for RBF neural networks.

 Around 200 neurons and training points were necessary for good ten-port calibration. With these conditions the RBF learning procedure was able to produce good estimations of both the magnitude and phase of the reflection coefficient without needing any phase lock device.

1
2
3
4
5
6
7
8
9
10
11
12
13
14
15
16
17
18
19
20
21
22
23
24
25
26
27
28
29
30
31
32
33
34
35
36
37
38
39
40
41
42
43
44
45
46
47
48
49
50
51
52
53
54
55
56
57
58
59
60

ACKNOWLEDGEMENTS

REFERENCES

1. A. C. Metaxas and R. J. Meredith, Industrial Microwave Heating, Peter Peregrinus Ltd., London, 1983.
2. G. Colef, P. R. Karmel, and M. Ettenberg, New in-situ calibration of diode detectors used in six-port network analyzers, IEEE Trans Instrum Meas 39 (1990), 201–204.
3. E. J. Griffin, Six-port reflectometer circuit comprising three directional couplers, Electron Lett 18 (1982), 491–493.
4. C. A. Hoer, The six-port coupler: a new approach to measuring voltage, current, power impedance and phase, IEEE Trans Instrum Meas 21 (1972), 466–470.
5. G. F. Engen, The six-port reflectometer: an alternative network analyzer, IEEE Trans Microwave Theory Tech 25 (1977), 1075–1080.
6. G. F. Engen, A least squares solution for use in the six-port measurement technique, IEEE Trans Microwave Theory Tech 28 (1980), 1473–1477.
7. J. Monzó-Cabrera, J. L. Pedreño-Molina, A. Lozano-Guerrero, and A. Toledo-Moreo, A novel design of a robust ten-port microwave reflectometer with autonomous calibration by using neural networks, IEEE Trans Microwave Theory Tech 56 (2008), 2972–2978.
8. J. L. Pedreño-Molina, J. Monzó-Cabrera, A. Lozano-Guerrero, and A. Toledo-Moreo, Design and validation of a ten-port waveguide reflectometer sensor: application to efficiency measurement and optimization of microwave-heating ovens, Sensors 8 (2008), 7833–7849.

LIST OF CAPTIONS

Figure 1   Scheme for the measurement set-up used in this work

Figure 2   Scheme and dimensions of the proposed impedance generator: a) main view and b) side view. All dimensions in cm

Figure 3   Experimental set-up used during the ten-port calibration and validation procedures
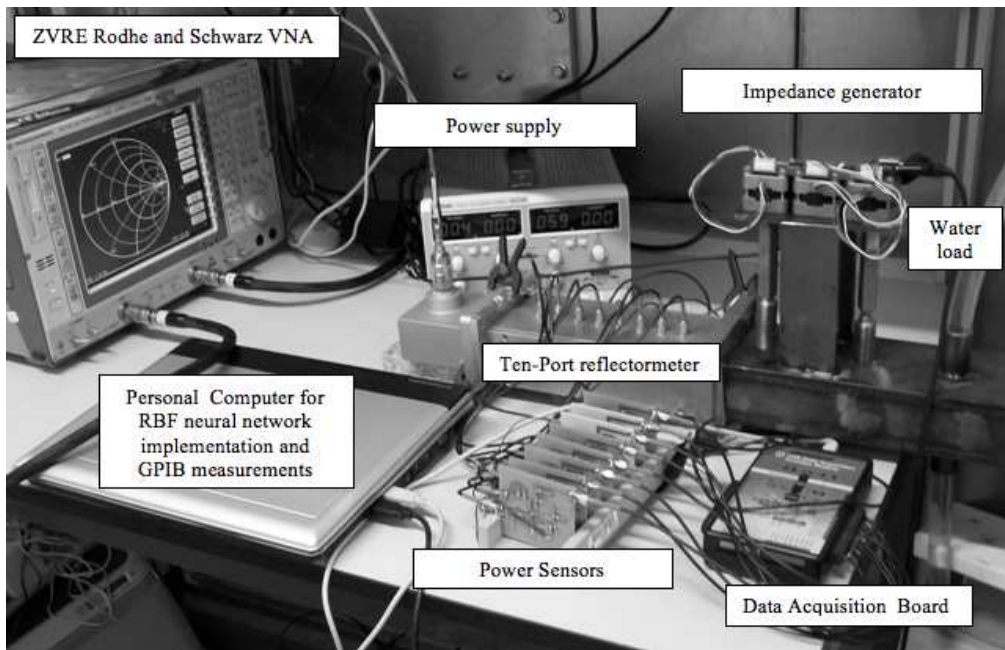
Figure 4   Reflection coefficient values measured by the VNA for different positions of the three automated stubs

Figure 5   Reflection coefficient data employed for RBF training (black points) and RBF validation (grey points)

Figure 6   Comparison of $|S_{11}|$ reference value (measured with VNA) and ten-port measurement

Figure 7   Comparison of S_{11} phase reference value (measured with VNA) and ten-port measurement
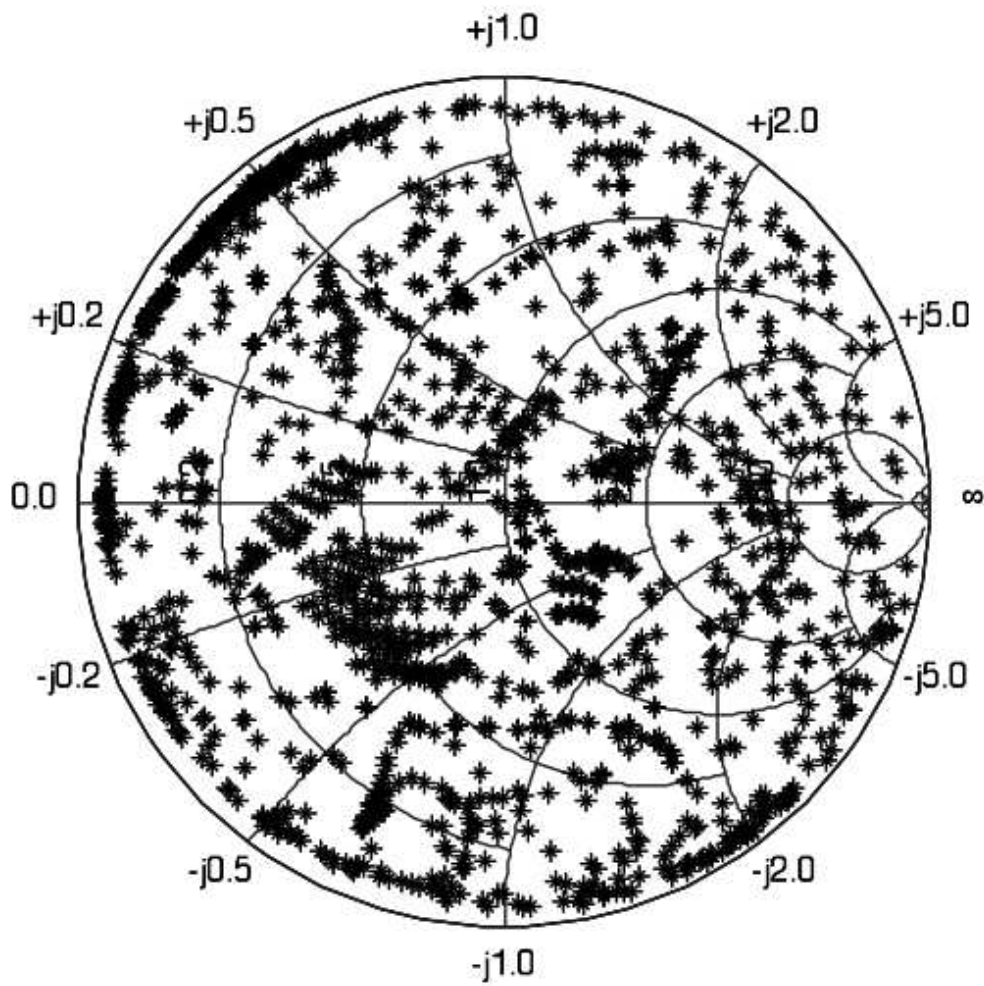
1
2
3
4
5
6
7
8
9
10
11
12
13
14
15
16
17
18
19
20
21
22
23
24
25
26
27
28
29
30
31
32
33
34
35
36
37
38
39
40
41
42
43
44
45
46
47
48
49
50
51
52
53
54
55
56
57
58
59
60

311x146mm (72 x 72 DPI)

212x192mm (72 x 72 DPI)

225x144mm (72 x 72 DPI)
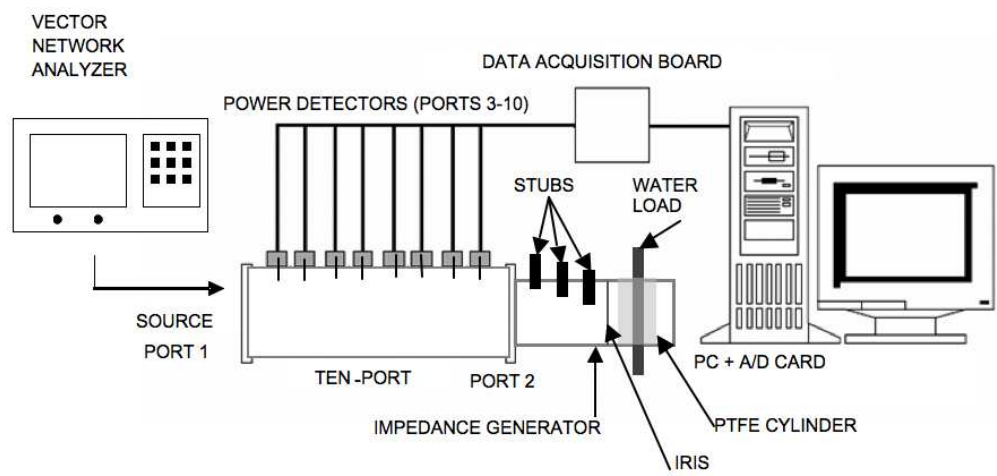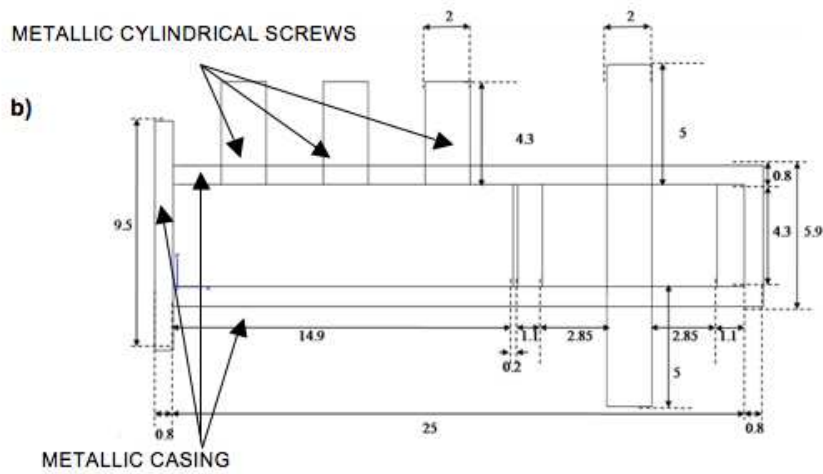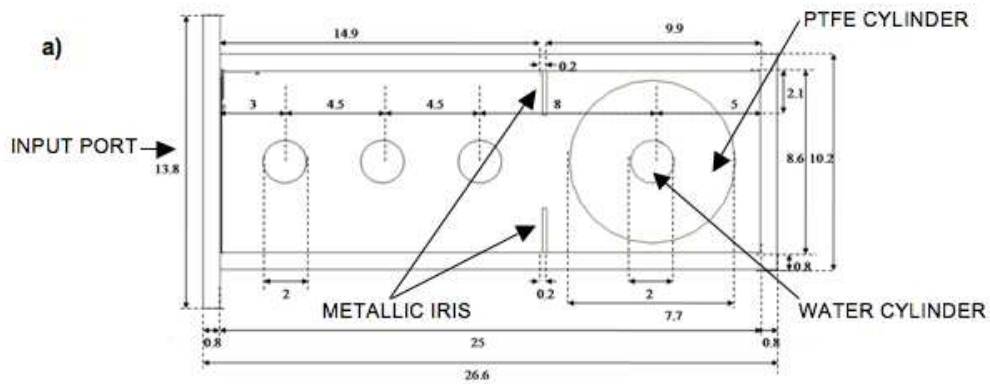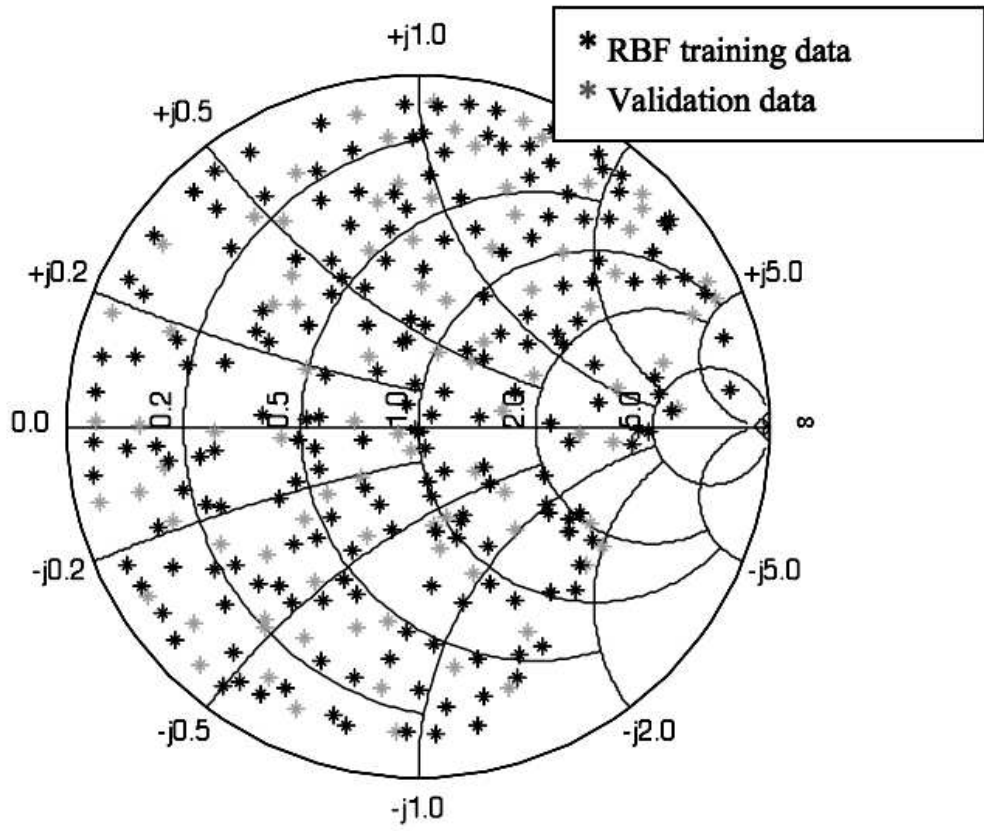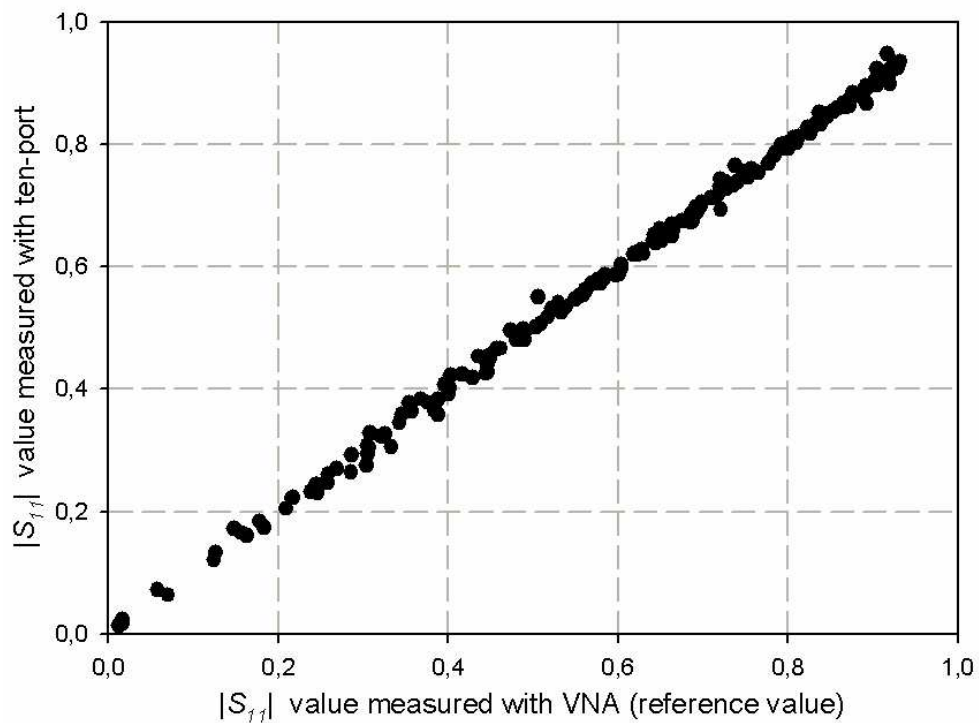
179x177mm (72 x 72 DPI)

1
2
3
4
5
6
7
8
9
10
11
12
13
14
15
16
17
18
19
20
21
22
23
24
25
26
27
28
29
30
31
32
33
34
35
36
37
38
39
40
41
42
43
44
45
46
47
48
49
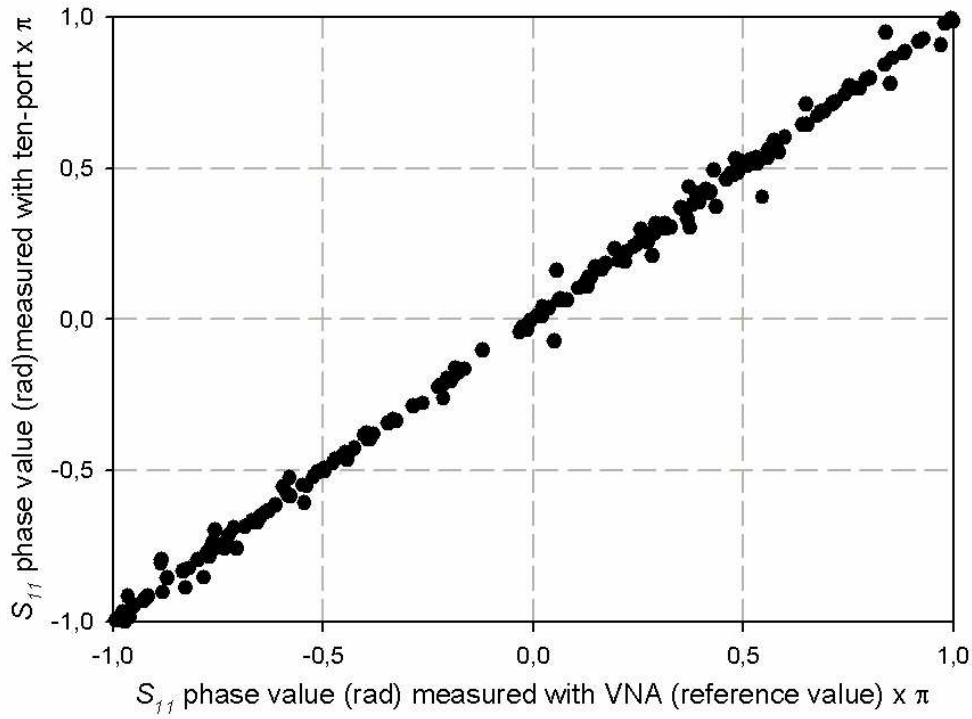50
51
52
53
54
55
56
57
58
59
60

227x192mm (72 x 72 DPI)

147x117mm (150 x 150 DPI)

148x118mm (150 x 150 DPI)